Effects of the graphene nanoplatelets reinforced interphase on mechanical properties of carbon fibre reinforced polymer – a multiscale modelling study.

Marzena Pawlik [a], Huirong Le [a], Yiling Lu [a, 1]

[a] School of Mechanical Engineering and Built Environment,

College of Engineering and Technology,

University of Derby, Markeaton Street, Derby, DE22 3AW, UK

Abstract:

Mechanical properties of carbon fibre reinforced polymer (CFRP) are greatly affected by an interphase between fibre and matrix. Coating fibre with nanofillers has been suggested to improve the interphase properties. In this paper, a multiscale modelling framework was developed to investigate how graphene nanoplatelets (GnPs) influence the mechanical properties of CFRP laminate by reinforcing the interphase. At the nanoscale, the Mori-Tanaka homogenisation method was used to determine effective properties of the GnPs reinforced interphase. GnPs reinforced interphase properties at different GnPs orientations, and volume fractions were examined. At the microscale, a 3-D representative volume element (RVE) model based on obtained interphase properties was used to predict the elastic constants of CFRP unidirectional lamina. This RVE model consisted of three phases: carbon fibre, epoxy resin and the GnPs reinforced interphase. The incorporation of GnPs in the interphase increased both longitudinal and transverse lamina moduli. Finally, simulations of the three-point bending test were performed on the macroscale CFRP laminate. The macroscale modelling based on predicted lamina properties was found to reproduce experimentally measured flexural modulus well. It was found that the GnPs coating on fibre has a positive influence on the mechanical properties of CFRP, and the enhancement varied with orientation and local volume fraction of GnPs. In the presence of GnPs coating, 0° and 90° flexural moduli of CFRP laminate increased by 6.1% and 28.3% respectively.

Keywords:

Graphene nanoplatelets, fibre-reinforced composite, interphase, mechanical properties, multiscale modelling

[1] Corresponding author: y.lu@derby.ac.uk

1. Introduction

Carbon fibre reinforced composites have superior mechanical properties and excellent design flexibility [1]. Their mechanical performance is hugely affected by the interphase between carbon fibre and matrix [2]. This interphase layer plays an essential role in the effective load transfer between matrix and fibre and improves overall composite performance [3]. Recently coating fibres with nanofillers such as graphene or carbon nanotubes (CNTs) have shown huge potential in enhancing the interphase properties [4-14]. The GnPs coated CFRP laminate showed 52%, 7%, and 19% of increase compared with non-coated CFRP laminate, for 90° flexural strength, 0° flexural strength and interlaminar shear strength respectively [10]. Zhang et al. [16] observed a 12.7% enhancement of interlaminar shear strength after introducing graphene oxide sheets to the carbon fibre-matrix interphase.

Graphene is a 2-D flake shape material and behaves transversely isotropic. It has been applied to the fibre surface by dip coating [8–12], electrophoretic deposition [13–15] or chemical grafting [16]. The resultant interphase exhibits distinctive mechanical properties, which are affected by orientation, volume fraction and dispersion of graphene within the interphase [17]. The orientation of the graphene tends to be more random during dip coating of fibres in graphene-epoxy solution, whereas electrophoretic deposition or chemical grafting will make graphene more aligned along the fibre surface.

Quantitative characterisation of the interphase region remains challenging. It is commonly accepted that the interphase properties for the fibre-reinforced composite are somewhere between fibre and matrix [18]. Interphase modulus can be measured by nanoindentation, AFM or dynamic mechanical mapping [19,20]. For example, the interphase storage modulus of 60 GPa was measured using dynamic nanoscale imaging [19]. However,

these experimental measurement processes are very difficult to conduct due to the surface roughness, size-scale effects and tip blunting [21]. So far, there are no direct experimental measurements of the GnPs reinforced interphase properties.

Computational micromechanics is an alternative method to study the interphase problem, among which Representative Volume Element (RVE) is most widely used [22–31]. The interphase of traditional CFRP was usually treated as a cohesive layer zone [28] or a separate phase of defined thickness [24–27,32]. Effectively three phases: fibre, matrix and the interphase, were proposed in these studies. The interphase can be depicted by either homogeneous [24–26] or inhomogeneous [23,32] material model. Several studies on fuzzy fibre reinforced polymer (FFRP) were recently reported [33–38]. In FFRP, CNTs nanofillers were radially grown on fibres, which in turns dictated the thickness and mechanical properties of the whole interphase. Effective properties of the CNTs reinforced interphase were calculated by the mechanics of materials [33], the RVE nanoscale model [34], composite cylinder method [35] or Mori-Tanaka method [39]. Chatzigeorgiou et al. [35] investigated the effects of CNTs volume fraction and length on the mechanical properties of CFRP. A significant improvement in composite moduli (exceeding 200%) was observed in the transverse direction of the fuzzy fibre.

Simulations work of CFRP reinforced with nanofillers of 2-D sheet structure is rather limited. Few papers studied the fibre reinforced polymers with graphene either introduced in the matrix or on the fibre surface [40,41]. Dai and Michnaevsky [42] analysed fatigue damage of fibre reinforced polymer reinforced with nanoclay particles. Nanoclay was introduced to modify matrix or the interphase. The highest improvement in fatigue life was observed when nanoclay was located in the interphase between fibre and matrix. Recently Sabuncuoglu et al. [3] studied stress concentration within steel fibre composite with nano-reinforced interphase under transverse loading. The primary challenge of the FEA of the

FRPs reinforced with graphene is the difference in dimensions of nanoscale graphene, microscale fibre, and macroscale laminate. The behaviour of these materials has to be simulated at multiple scales, resulting in a more complex analysis.

A multiscale modelling approach was used to quantify the effects of orientations and volume fractions of GnPs on the mechanical properties of CFRP laminate as described in **Section 2**. At the nanoscale, the effective properties of GnPs reinforced interphase were calculated using the Mori-Tanaka method. At the microscale, the CFRP lamina elastic constants were obtained from RVE analysis. The influence of the GnPs volume fraction and orientation on lamina elastic constants was established. Finally, three-point bending was simulated at the macroscale level. The results were compared with published experimental data in **Section 3** and discussed in **Section 4**.

2. Multiscale modelling approach

2.1 Nanoscale modelling

2.1.1 Determination of the interphase properties using the Mori-Tanaka method

Mori-Tanaka method [43,44] was used to estimate properties of nanocomposite [45,46], and recently also applied to predict properties of the CNTs [36] and the graphene [3] reinforced interphase in fibre reinforced composites. To simplify the mathematical expression of the Mori-Tanaka method, Hills' parameters: *k, l, n, m* and *p* were utilised. For each constituent or the whole mixture, these Hill's parameters can be interconverted to elastic properties. GnP is of disc shape and behaves transversely isotropic. It is described by a local coordinate system with the 1'-2' plane of isotropy and axis 3' being through-the-thickness direction (**Figure 1a**). GnP's elastic properties are referred to as equation (1) in terms of Hill's parameters:

$$E_{1'}^{r} = \frac{4m_r(k_r n_r - {l_r}^2)}{(k_r + m_r)n_r - {l_r}^2}$$

$$E_{3'}^{r} = n_r - \frac{{l_r}^2}{k_r}$$

$$G_{1'3'}^{r} = p_r$$

$$v_{1'2'}^{r} = \frac{(k_r - m_r)n_r - {l_r}^2}{(k_r + m_r)n_r - {l_r}^2}$$

$$v_{1'3'}^{r} = \frac{l_r}{2k_r} \quad (1)$$

Note that throughout the paper subscripts, *r* and *m* represent reinforcement GnPs and epoxy matrix respectively, and superscript *I* denotes interphase. Epoxy is isotropic, and its Hill's parameters can be related to elastic properties by equation (2).

$$k_m = \frac{E^m}{2(1+v^m)(1-2v^m)}$$

$$l_m = \frac{v^m E^m}{(1+v^m)(1-2v^m)}$$

$$m_m = p_m = \frac{E^m}{2(1+v^m)}$$

$$n_m = \frac{(1-v^m)E^m}{(1+v^m)(1-2v^m)} \quad (2)$$

The interphase properties are affected by the orientation of nanofillers, which in turn is dependent on the technique of coating GnPs onto the fibre surface. Both random and aligned orientations are compared (see **Figure 1b** and **1c**). All GnPs assume even distribution in the reinforced interphase. Once GnPs and matrix Hill's parameters are known, the properties of the GnPs reinforced interphase can be then calculated. The derivation of equations 1-6 can be found elsewhere [44].

2.1.2 Aligned GnPs in the reinforced interphase.

According to the aligned orientation, GnPs are located parallel to the fibre surface wrapping around the fibre (**Figure 1b**). This orientation causes the GnPs reinforced

interphase to behave in a transversely isotropic manner. Following a similar local coordinate system to single GnP, the Hill's parameter of the interphase are calculated as follow:

$$k^I = V_r k_r + V_m k_m - \frac{V_m V_r (l_r - l_m)^2}{V_r n_m + V_m n_r}$$

$$l^I = \frac{V_r l_r n_m + V_m l_m n_r}{n_r V_m + n_m V_r}$$

$$m^I = V_r m_r + V_m m_m$$

$$n^I = \frac{n_m n_r}{V_r n_m + V_m n_r}$$

$$p^I = \frac{p_m p_r}{V_r p_m + V_m p_r} \quad (3)$$

where V_r and V_m represent volume fraction of GnPs and epoxy matrix respectively. The interphase elastic properties are interconverted from equation (3):

$$E^I_{1'} = \frac{4m^I(k^I n^I - {l^I}^2)}{(k^I + m^I)n^I - {l^I}^2}$$

$$E^I_{3'} = n^I - \frac{{l^I}^2}{k^I}$$

$$G^I_{1'3'} = p^I$$

$$v^I_{1'2'} = \frac{(k^I - m^I)n^I - {l^I}^2}{(k^I + m^I)n^I - {l^I}^2}$$

$$v^I_{1'3'} = \frac{l^I}{2k^I} \quad (4)$$

where $E^I_{1'}$, $E^I_{3'}$, $G^I_{1'3'}$, $v^I_{1'3'}$, $v^I_{1'2'}$ are defined as in-plane elastic modulus, out-of-plane elastic modulus, out-of-plane shear modulus, out-of-plane Poisson's ratio, in-plane Poisson's ratio of the interphase respectively.

2.1.3 Randomly orientated GnPs in the reinforced interphase.

When GnPs are randomly distributed in the coating (**see Figure 1c**), the GnPs reinforced interphase behaves in the isotropic way even GnPs are transversely isotropic [44]. As a result, the interphase properties can be represented entirely by a set of two

parameters (E^I, v^I *or* κ^I, μ^I). Following the Mori-Tanaka method, bulk (κ^I) and shear (μ^I) moduli of the GnPs reinforced interphase can be found by equation (5) then converted to Young's modulus (E^I) and Poisson's ratio (v^I) in equation (6) accordingly. Detailed expression of intermediated variables ($\alpha, \beta, \delta, \eta$) are provided in reference [44].

$$\kappa^I = \kappa^m + \frac{V_r(\delta - 3\kappa^m\alpha)}{3(V_m + V_r\beta)}, \mu^I = \mu^m + \frac{V_r(\eta - 2\mu^m\beta)}{2(V_m + V_r\beta)} \quad (5)$$

$$E^I = \frac{9\kappa^I\mu^I}{3\kappa^I + \mu^I}, v^I = \frac{3\kappa^I - E^I}{6\kappa^I} \quad (6)$$

2.1.4 Material parameters for GnPs reinforced interphase

Due to the difficulties in experimental measurements, there exists a wide range of variation in the properties of GnPs and graphene sheets in the literature [3,40,42,45,47–51]. Unlike previous nanoscale models assuming graphene isotropic [42,48], this study takes its transversely isotropic features into account to more realistically represent the effects of the GnPs reinforced interphase. In-plane properties of graphene are usually measured by AFM nanoindentation. Graphene in-plane elastic modulus ranges from 300.0 GPa [52] to 1.0 TPa [51]. It is more challenging to determine graphene's out-of-plane properties in through-the-thickness direction, which are not even provided by material suppliers [53]. Molecular dynamics simulation is an alternative way to establish missing information on those properties [45]. Properties of GnPs and isotropic resin 828 are summarised in **Table 1**.

It is nearly impossible to measure the local volume fraction of nanofillers at the interphase experimentally. A range of local volume fractions of CNTs from 0 to 80% was used by one parametric numerical study [35]. In the present study, the volume fraction of GnPs assumes the range from 0 to 60%. Interaction among GnPs was not considered at this stage.

2.2 Microscale modelling

2.2.1 RVE method

RVE method was used to investigate the effects of the GnPs reinforced interphase on the lamina's properties. Fibres were assumed to be uniformly embedded in the matrix (**Figure 2a**). Although fibre distribution is not always regular across the cross-section, the periodic fibre arrangement has proved to be a good approximation [22–26]. The present RVE model adopted a hexagonal array of fibre sequence (**Figure 2b**), where the lamina always exhibits a transversely isotropic feature. A local coordinate system was adopted for the lamina with 1-axis aligned with the fibre direction. Elastic constants of the lamina were determined from Hooke's law using volume average strains and stresses when the RVE was loaded in some prescribed ways [54]. A complete set of elastic properties were obtained for transversely isotropic CFRP lamina: E_1 and E_2 represent the longitudinal and transverse moduli, G_{12} and G_{23} are longitudinal and transverse shear moduli, v_{12} is longitudinal Poisson's ratio respectively. The comprehensive description on the RVE method can be found elsewhere [54–56].

2.2.2 Parameters for the present RVE model

This present study investigated the same AS4/EPON 828 lamina, which was used to make laminate samples in published experimental work [10]. The volume fraction of carbon fibres was fixed at 66%. Height, width and thickness of the RVE model dimension were calculated as $7.20, 4.16$ and 1.04 μm respectively [54]. Properties of a transversely isotropic carbon fibre AS4 and isotropic epoxy resin 828 were taken from the literature [51,59] (see **Table 1**). The GnPs reinforced interphase thickness was estimated as 200 nm. This value was derived from SEM image analysis (see Figure 3 in [10]). The volume fractions of each constituent in the RVE models were 66%, 26.3% and 7.7% for carbon fibre, epoxy and GnPs reinforced interphase respectively. The interphase properties obtained from the nanoscale

model were input to this RVE model. The RVE model was simulated using ANSYS APDL 18.0 (ANSYS Inc., UK). Two orientations of GnPs (random and aligned) were compared. The aligned GnPs reinforced interphase is transversely isotropic. The material properties assigned to the interphase layer in the RVE model are better-implemented using a local coordinate system. The orientation of each element in the interphase layer was defined using VEORIENT [58]. The circumference of the carbon fibre was chosen as the line option. As a result, the normal direction of each interphase element followed the direction of the neighbouring surface on the carbon fibre. The validation and mesh independent test of this RVE method was accomplished with the published fuzzy fibre model [37].

2.3 Macroscale modelling

The effectiveness of this multiscale approach was further proved in the macroscale model, where experimental data was available. Three-point bending test was simulated to study the effects of the GnPs reinforced interphase on flexural modulus of the CFRP laminate to mimic the experiment performed by Qin et al. [10]. Qin et al. reported a dense layer of homogeneously dispersed GnPs on the carbon fibre surface, which makes the random orientated model of the interphase more suitable for the comparison purpose. Based on the available sample preparation quantitative details, the local volume fraction of GnPs in the reinforced interphase was estimated to be 20%. Corresponding lamina properties from the microscale model (**Section 2.2.2**) were used for analysis and provided in **Table 2**. For the control samples where there is no GnPs coating, the fibre volume fraction was 65%, which was also the same as the experiment [10].

The macroscale FEA model was implemented using Ansys Workbench 18.0 (Ansys Inc., UK). A 12-layer unidirectional laminate model used the dimensions of 100 mm, 12.7 mm, and 2.3 mm replicating the reported experiment [10]. The laminate was built in the software using a layered section command, which passed the validation and mesh

independent test. To simulate the three-point bending test, the vertical force was applied in the middle of the sample. Simply supported boundary condition was assigned with a span length of 80 mm for the numerical model. The displacement was recorded from the middle point of the sample span, a flexural modulus of this material was calculated using equation (7) [60]. The numerical results were then compared with published experimental data in **Section 3.3**.

$$E_f = \frac{L^3}{4bh^3}\frac{\Delta F}{\Delta s} \quad (7)$$

3. Results

3.1 Properties of the GnPs reinforced interphase

Figure 4 presents the relationship between the interphase's mechanical properties against the volume fraction of GnPs within the interphase. When the volume fraction of GnPs is nil, the interphase Young's modulus is equal to that of the pure resin matrix, i.e. 3.45 GPa. In the presence of randomly orientated GnPs, Young's modulus of the GnPs reinforced interphase increases monotonically with the volume fraction of GnPs (**Figure 4a**). While the Poisson's ratio of the interphase decreases to 0.19 at 9% of the volume fraction of GnPs then increases monotonically with the volume fraction, as shown in **Figure 4b**. For the highest volume fraction GnPs being studied, i.e. 60%, Young's modulus of the interphase is predicted 370.5 GPa and the Poisson's ratio 0.42.

When GnPs are perfectly aligned in the interphase with the fibre direction, the interphase is transversely isotropic (**Figure 5**). The in-plane elastic modulus of the interphase increases quasi-linearly with the volume fraction of GnPs (**Figure 5a**). Compared to the case of the random orientation of GnPs, the increase in Young's modulus is significantly higher when the volume fraction of GnPs introduced to the fibre surface is over 10%. The ratio of in-plane Young's modulus of random orientation interphase to perfectly aligned interphase

varies from 0.57 to 0.8 in the range of volume fraction of GnPs being tested. **Figure 5d** shows that in-plane shear modulus of this interphase exhibits a similar increase with the volume fraction of GnPs. Moreover, the increase of this modulus in the perfectly aligned GnPs in the interphase is constantly higher than the interphase with GnPs random distribution.

The out-of-plane elastic modulus of the interphase exhibits a sigma-like increase with the volume fraction of GnPs, as shown in **Figure 5b**. This modulus increases from 3.45 GPa for pure matrix up to 12.7 GPa for 60% volume fraction of GnPs. The out-of-plane shear modulus increases from 1.2 GPa to 3.1 GPa (**Figure 5c**). This shear modulus is two orders of magnitude lower than that of randomly orientated GnPs, which can be calculated from given elastic modulus and Poisson's ratio. The in-plane shear modulus increases nearly linearly from 3.45 to 224 GPa for the given volume fraction range.

3.2 The effects of GnPs reinforced interphase on the CFRP lamina elastic constants.

The interphase properties obtained in **Section 3.1** were input to the RVE model. The volume fraction of GnPs varied from 0 to 60% parametrically, which is relative to the interphase only. Two orientations of GnPs (random and aligned) were compared in order to illustrate the influence of the GnPs reinforced interphase on lamina elastic constants.

3.2.1 Longitudinal and transverse moduli.

Figure 6 shows the change of the lamina elastic moduli. For 0% GnPs volume fraction, the interphase properties are equal to that of epoxy resin. Therefore, the longitudinal and transverse Young's moduli of the 66% carbon and 34% epoxy resin are 149.3 and 9.1 GPa respectively. This is used as the baseline of CFRP lamina.

Both aligned and randomly orientated GnPs coatings moderately improve longitudinal Young's modulus (E_1) as presented in **Figure 6a**. E_1 increases nearly linearly with the volume fraction of GnPs for the case of aligned GnPs within the interphase. While the case of

randomly orientated GnPs presents a somewhat nonlinear increase of E_1. The improvement is slightly higher for aligned GnPs in the interphase, but the difference in the enhancement between aligned and randomly orientated GnPs is no more than 8.0 GPa. For example, the lamina longitudinal modulus increases from 149.3 GPa for baseline CFRP to 185.3 GPa for 60% aligned GnPs in the reinforced interphase. For the same volume fraction of randomly orientated GnPs, this is about 7.0 GPa lower.

Figure 6b presents the relation of lamina transverse modulus (E_2) versus GnPs volume fraction within the interphase. When GnPs are aligned in the reinforced interphase, a rapid improvement of 8% is observed with as low as 4% of GnPs. Further increase of GnPs yields little enhancement. On the other hand, randomly orientated GnPs in the interphase shows a similar increase to the aligned case for up to 4% of GnPs in volume fraction. Above this value, a continuously noticeable linear growth of E_2 with the GnPs content is found. For 60% GnPs in the reinforced interphase, lamina transverse modulus increases from 9.2 GPa for the baseline CFRP to 12.0 GPa and 10.5 GPa for randomly orientated and aligned case respectively.

3.2.2 Longitudinal and transverse shear moduli

Both shear moduli were enhanced due to the introduction of GnPs in the interphase (**Figure 7**). GnPs orientation affects the changing trend of in-plane shear moduli. For aligned and randomly orientated GnPs in the reinforced interphase, up to 2% volume fraction brisk increase of shear moduli is observed. After that, the aligned GnPs case shows little change with a further increase in the volume fraction of GnPs. On the contrary, the randomly orientated case has shown continuous, but slow increments of moduli. G_{12} increases from 5.2 GPa (0% GnPs volume fraction) to 7.1 GPa (60% GnPs volume fraction). The difference between random and aligned orientations in G_{12} values is 0.3 GPa (for 60% GnPs volume

fraction). Lamina transverse shear modulus (G_{23}) increases from 3.1 GPa (baseline CFRP) to 3.9 GPa, and 3.5 GPa for 60% randomly orientated and aligned GnPs respectively.

3.2.3 Poisson's ratio

For the completeness of results, **Figure 8** presents the effects of the GnPs reinforced interphase on the Poisson's ratio of the unidirectional lamina. For aligned GnPs, v_{12} of the lamina shows little difference in comparison to the Poisson's ratio of the baseline CFRP. Longitudinal Poisson's ratio for randomly orientated case remain unchanged up to 20% of GnPs in the interphase and starts growing gradually with the further increase of volume fraction of GnPs.

3.3 Flexural modulus of CFRP laminate with the GnPs reinforced interphase.

Four types of laminates made of 12 unidirectional laminas were numerically modelled to reproduce the three-point bending experiment. An example of the contour plot of vertical directional deformation of 0° unidirectional lamina at a loading of 700 N is shown in **Figure 9**. Due to the simple geometry and loadings, the resultant deformation is uniform across the width of the laminate. Maximum downwards displacement occurred to the middle point of this sample while its both free ends experienced upwards deflections. Sample dimensions provided in section 2.3, applied force and corresponding maximum displacement were entered into equation (7) to calculate the flexural modulus (E_f). The comparison between predicted E_f using the present methodology and experimental measurement [10] is provided in **Table 3**. Calculated flexural modulus for 0° unidirectional laminate with GnPs coated on the fibre was 152.1 GPa and is within the range of experimental measurements 143$\pm$9.0 GPa. The predicted value of 90° flexural modulus for GnPs coated laminate (11.9 GPa) was found very close to the experimental value of 11.0 $\pm$0.3 GPa. The numerical modelling was able to predict flexural modulus of CFRP laminate satisfactorily. Both samples without GnPs

reinforced interphase showed good agreement with experimental results. The average percentage error in flexural moduli of all predicted laminates was below 3%.

4. Discussion

A complete set of properties of the GnPs reinforced interphase was for the first time calculated by taking into account transversely isotropic features of GnPs. The interphase is essentially a thin layer of GnPs nanocomposite. The interphase's volume fraction to the whole CFRP composite is 7.7% and at a high local volume fraction of GnPs in the interphase, i.e. 60%, the resultant volume fraction of GnPs in the whole composite is 4.6%. This volume fraction is comparable to that of other nanocomposites studies [16]. However, unlike nanocomposites, where nanofillers are dispersed throughout the composite, the present CFRP reinforced by GnPs has all nanofillers concentrated on the fibre surface, which only reinforces the interphase layer. Properties of GnPs reinforced interphase determined in the present study can be correlated with published values of nanocomposites [44,46]. In the GnPs nanocomposite, the elastic modulus of randomly orientated GnPs nanocomposite was reported 0.53 of that of the aligned case at low volume fractions of GnPs [61]. The ratio of the interphase elastic modulus for two GnPs orientations from the present simulation is close to this value. Although most nanocomposite studies only focused on the elastic modulus [44,62], the increase in shear modulus of the interphase with GnPs was also predicted. This directly supports speculation given by [10] that the shear modulus of the interphase region increases with GnPs coating.

The extent of the lamina properties enhancement depends highly on the orientation of GnPs within the interphase. CFRP lamina always exhibits high longitudinal properties due to the fibre's high longitudinal modulus. GnPs coating on the fibre improved longitudinal elastic modulus (E_1) of the CFRP lamina moderately. When all GnPs at a local volume fraction of 20% in the interphase were randomly orientated, E_1 was increased by 4.6%, compared with

the baseline CFRP model. When these GnPs were aligned in the interphase, the increase in E_1 was even higher (i.e. 7.9%). This can be explained as follows, when GnPs orientations are parallel to the fibre surface, exceptionally high in-plane moduli of GnPs are fully exploited via a higher E_1^I, possessed by the interphase.

Unlike the moderate effects on longitudinal modulus, the transverse modulus E_2 for the CFRP lamina is much more sensitive to the orientation of GnPs in the interphase. Based on the same local GnPs content in the interphase (20%), the increase of E_2 for the randomly orientated case was as high as 22.6%. However, when the same amount of GnPs became aligned, the enhancement of resultant lamina modulus was only 10%. Randomly orientated GnPs endows the isotropic properties of the interphase. Therefore, the remarkable in-plane properties of GnPs were utilised in all directions. On the contrary, the out-of-plane properties of the GnPs aligned interphase were much weaker. This indicates that unifying GnPs orientation parallel to the fibre surface may not yield maximum beneficial improvement in terms of transverse material properties. All these quantitative analyses filled in the knowledge gap in the material properties of GnPs reinforced CFRP lamina.

The GnPs reinforced CFRP proposed in this study is somehow similar to the fuzzy fibre reinforced composite as both make use of nanofillers reinforcement in the interphase. Chatzigeorgiou et al. [35] observed that reinforced interphase did not change the longitudinal properties, but improved the transverse properties of fuzzy fibre reinforced composite significantly by 200%. In the fuzzy fibre reinforced composite, the axial direction of CNTs growing on the fibre surface is in line with the fibre transverse direction. This may represent the maximum enhancement possible for this type of interphase. According to the findings in fuzzy CFRP, maximum GnPs reinforcement to CFRP may be achieved at the orientation of GnPs perpendicular to the fibre surface. This type of graphene alignment has been already

implemented in sensors, fuel cells and supercapacitors [63]. Resultant interphase in fuzzy fibre composite is unusually thick (~ 2 μm), which is dictated by the full length of CNTs.

A 12-layer CFRP laminate with carbon fibres coated with GnPs was simulated in the three-point bending configuration to determine the flexural properties. The laminate deformation and resultant stress distribution were obtained. Predicted flexural modulus of four different types of laminates was compared with published experimental data [10]. 90° flexural moduli were calculated as 8.7 and 11.2 GPa for baseline CFRP and GnPs reinforced CFRP respectively. Both 90° flexural moduli of CFRP without GnPs agreed well with the counterpart of experimental data 8.8 $\pm$ 0.3 MPa and 11.0 $\pm$ 0.3 MPa. The difference between numerical prediction and experiment is below 1%. By contrasting the baseline CFRP, reinforcement of GnPs led to a 28.3% enhancement in 90° flexural modulus, whereas the improvement in 90° flexural modulus achieved by experimental studies was 25% [10]. 0° flexural moduli 143.2 and 152.1 GPa were calculated for baseline CFRP and GnPs reinforced CFRP respectively. These values matched reasonably well the range of experimental data (139$\pm$3.0 GPa for baseline CFRP, 143$\pm$9.0 GPA for GnPs reinforced CFRP). The slight overestimation was mainly caused by the assumption of regular distribution of fibres in the present microscale RVE model. Other RVE modelling work based on the same assumption also reported a similar discrepancy with that of randomly distributed modelling [24,29]. The presence of GnPs caused the 6.1% improvement in 0° flexural modulus from this multiscale modelling.

Besides the improvement in elastic properties of CFRP as shown in this study, the GnPs coating will increase other mechanical properties such as fracture toughness, interfacial and interlaminar shear strength [10,13,15]. Chemical reactions and mechanical interlocking processes increase the bonding between the matrix and fibre. Fibres coated with graphene increase their surface roughness and surface morphologies [13], which are believed to

enhance interfacial adhesion. The 90° flexural properties have been reported most sensitive to this enhancement [64], which was confirmed in our simulations.

There are some limitations to this work. GnPs are assumed straight and evenly distributed in the interphase. However, as the local volume fraction of GnPs increases to a threshold value, GnPs agglomeration due to the Van der Waals forces [17] could become non-negligible, and interaction between GnPs should be taken into account. During the manufacturing process, some imperfections are unavoidable. This approach neglects the production flaws such as voids, cracks and delamination. Future improvement in this modelling work needs to address these issues.

5. Conclusion

In conclusion, a multiscale model was developed to study the effects of the GnPs reinforced interphase on the elastic properties of CFRP laminate. The effective material properties of the reinforced interphase were determined by considering transversely isotropic features of GnPs. The presence of GnPs in the interphase enhances the elastic properties of CFRP lamina, and the enhancement depends on its volume fraction. Randomly orientated GnPs in the interphase yields a higher improvement in transverse properties of the composite. The present multiscale modelling was able to reproduce experimental measurements for GnPs reinforced CFRP laminates well. To the best of the authors' knowledge, this is the first time the effects of orientation and volume fraction of GnPs coated on the fibre surface on elastic constants of CFRP was numerically quantified at different scales. This multiscale model could be potentially used to inversely quantify the interphase properties by combining with some standard material testing.

Acknowledgements

Marzena Pawlik is supported by graduate teaching assistant funding from the College of Engineering and Technology at the University of Derby

Declaration of interest

The authors declare no conflict of interest.

Appendix: list of symbols

$\overline{\sigma}$	Volume average stresses
$\overline{\varepsilon}$	Volume average strains
V	Volume of the Representative Volume Element
E_1	Lamina longitudinal modulus
E_2	Lamina transverse modulus
G_{12}	Lamina longitudinal shear modulus
G_{23}	Lamina transverse shear modulus
v_{12}	Lamina longitudinal Poisson's ratio
k	Plane-strain bulk modulus for lateral dilatation without longitudinal extension
l	Cross modulus
m	Rigidity modulus for shearing in any transverse direction
n	Modulus for longitudinal uniaxial straining
p	Rigidity modulus for shearing in the longitudinal direction
$E_{1'}^{r}$	In-plane modulus of graphene nanoplatelet
$E_{3'}^{r}$	Out-of-plane modulus of graphene nanoplatelet
$G_{1'3'}^{r}$	Out-of-plane shear modulus of graphene nanoplatelet
$v_{1'2'}^{r}$	In-plane Poisson's ratio of graphene nanoplatelet
$v_{1'3'}^{r}$	Out-of-plane Poisson's ratio of graphene nanoplatelet
k_r	Graphene nanoplatelet plane-strain bulk modulus under lateral dilatation in the (1',2') plane
n_r	Graphene nanoplatelet modulus under uniaxial tension in 3' direction
l_r	Graphene nanoplatelet cross modulus
m_r	Graphene nanoplatelet shear modulus in the (1',2') plane
p_r	Graphene nanoplatelet shear modulus in the (1',3') or (2',3') plane
E^m	Elastic modulus of matrix EPON 828
v^m	Poisson's ratio of matrix EPON 828
κ^m	Bulk modulus of matrix EPON 828
μ^m	Shear (or rigidity) modulus of matrix EPON 828
k_m	Matrix plane-strain bulk modulus
l_m	Matrix cross modulus
m_m	Matrix shear modulus
p_m	Matrix shear modulus
n_m	Matrix modulus for longitudinal uniaxial straining
V_r	Volume fraction of GnPs in the reinforced interphase
V_m	Volume fraction of matrix in the reinforced interphase
α	Dimensionless parameter of Mori-Tanaka method for randomly orientated GnPs
β	Dimensionless parameter of Mori-Tanaka method for randomly orientated GnPs
δ	Dimensionless parameter of Mori-Tanaka method for randomly orientated GnPs
η	Dimensionless parameter of Mori-Tanaka method for randomly orientated GnPs
κ^I	Effective bulk modulus of randomly orientated GnPs reinforced interphase
μ^I	Effective shear (or rigidity) modulus of randomly orientated GnPs reinforced interphase
E^I	Elastic modulus of the randomly orientated GnPs reinforced interphase
v^I	Poisson's ratio of the randomly orientated GnPs reinforced interphase
$E_{1'}^{I}$	In-plane elastic modulus of the aligned GnPs reinforced interphase
$E_{3'}^{I}$	Out-of-plane elastic modulus of the of the aligned GnPs reinforced interphase
$G_{1'3'}^{\mathrm{I}}$	Out-of-plane shear modulus of the aligned GnPs reinforced interphase
$v_{1'3'}^{I}$	Out-of-plane Poisson's ratio of the of the aligned GnPs reinforced interphase
$v_{1'2'}^{I}$	In-plane Poisson's ratio of the aligned GnPs reinforced interphase
E_f	Flexural modulus

b Width of the macroscale specimen
h Thickness of the macroscale specimen
L Span length in three-point bending test
s Deflection of the sample in three-point bending test
F Force applied to the middle of sample in three-point bending test

References

[1] Kaw AK, Group F. Mechanics of Composite Materials. 2nd ed. Taylor & Francis Group; 2006.
[2] Kim J-K, Mai Y-W. Engineered interfaces in fiber reinforced composites. vol. 2. 1999. doi:10.1016/S1369-7021(99)80035-2.
[3] Sabuncuoglu B, Gorbatikh L, Lomov S V. Analysis of stress concentrations in transversely loaded steel-fiber composites with nano-reinforced interphases. Int J Solids Struct 2018;130–131:248–57. doi:10.1016/j.ijsolstr.2017.09.031.
[4] Zhao Z-G, Ci L-J, Cheng H-M, Bai J-B. The growth of multi-walled carbon nanotubes with different morphologies on carbon fibers. Carbon 2005;43:663–5. doi:10.1016/j.carbon.2004.10.013.
[5] Sager RJ, Klein PJ, Lagoudas DC, Zhang Q, Liu J, Dai L, et al. Effect of carbon nanotubes on the interfacial shear strength of T650 carbon fiber in an epoxy matrix. Compos Sci Technol 2009;69:898–904. doi:10.1016/j.compscitech.2008.12.021.
[6] Wood CD, Palmeri MJ, Putz KW, Ho G, Barto R, Catherine Brinson L. Nanoscale structure and local mechanical properties of fiber-reinforced composites containing MWCNT-grafted hybrid glass fibers. Compos Sci Technol 2012;72:1705–10. doi:10.1016/j.compscitech.2012.06.008.
[7] Jin SY, Young RJ, Eichhorn SJ. Hybrid carbon fibre-carbon nanotube composite interfaces. Compos Sci Technol 2014;95:114–20. doi:10.1016/j.compscitech.2014.02.015.
[8] Zhang X, Fan X, Yan C, Li H, Zhu Y, Li X, et al. Interfacial microstructure and properties of carbon fiber composites modified with graphene oxide. ACS Appl Mater Interfaces 2012;4:1543–52. doi:10.1021/am201757v.
[9] Chen L, Jin H, Xu Z, Shan M, Tian X, Yang C, et al. A design of gradient interphase reinforced by silanized graphene oxide and its effect on carbon fiber/epoxy interface. Mater Chem Phys 2014;145:186–96. doi:10.1016/j.matchemphys.2014.02.001.
[10] Qin W, Vautard F, Drzal LT, Yu J. Mechanical and electrical properties of carbon fiber composites with incorporation of graphene nanoplatelets at the fiber – matrix interphase. Compos Part B 2015;69:335–41. doi:10.1016/j.compositesb.2014.10.014.
[11] Ashori A, Rahmani H, Bahrami R. Preparation and characterization of functionalized graphene oxide/carbon fiber/epoxy nanocomposites. Polym Test 2015;48:82–8. doi:10.1016/j.polymertesting.2015.09.010.
[12] Knoll JB, Riecken BT, Kosmann N, Chandrasekaran S, Schulte K, Fiedler B. The effect of carbon nanoparticles on the fatigue performance of carbon fibre reinforced epoxy. Compos Part A 2014;67:233–40. doi:10.1016/j.compositesa.2014.08.022.
[13] Deng C, Jiang J, Liu F, Fang L, Wang J, Li D, et al. Influence of graphene oxide coatings on carbon fiber by ultrasonically assisted electrophoretic deposition on its composite interfacial property. Surf Coat Technol 2015;272:176–81. doi:10.1016/j.surfcoat.2015.04.008.
[14] Wang C, Li J, Sun S, Li X, Zhao F, Jiang B, et al. Electrophoretic deposition of graphene oxide on continuous carbon fibers for reinforcement of both tensile and interfacial strength. Compos Sci Technol 2016;135:46–53. doi:10.1016/j.compscitech.2016.07.009.
[15] Mahmood H, Vanzetti L, Bersani M, Pegoretti A. Mechanical properties and strain monitoring of glass-epoxy composites with graphene-coated fibers. Compos Part A Appl Sci Manuf 2018;107:112–23. doi:10.1016/j.compositesa.2017.12.023.
[16] Zhang RL, Gao B, Ma QH, Zhang J, Cui HZ, Liu L. Directly grafting graphene oxide onto carbon fiber and the effect on the mechanical properties of carbon fiber composites. Mater Des 2016;93:364–9. doi:10.1016/j.matdes.2016.01.003.
[17] Atif R, Inam F. Modeling and Simulation of Graphene Based Polymer Nanocomposites: Advances in the Last Decade. Graphene 2016;05:96–142. doi:10.4236/graphene.2016.52011.
[18] Kim J, Sham M, Wu J. Nano-scale characterisation of interphase in silane treated glass fibre composite. Composit Part A 2001;32. doi: 10.1016/S1359-835X(00)00163-9
[19] Gu Y, Li M, Wang J, Zhang Z. Characterization of the interphase in carbon fiber/polymer composites using a nanoscale dynamic mechanical imaging technique. Carbon 2010;48:3229–35. doi:10.1016/j.carbon.2010.05.008.

[20] Niu YF, Yang Y, Wang XR. Investigation of the interphase structures and properties of carbon fiber reinforced polymer composites exposed to hydrothermal treatments using peak force quantitative nanomechanics technique. Polym Compos 2018;39:E791–6. doi:10.1002/pc.24245.
[21] Hardiman M, Vaughan TJ, McCarthy CT. A review of key developments and pertinent issues in nanoindentation testing of fibre reinforced plastic microstructures. Compos Struct 2017;180:782–98. doi:10.1016/j.compstruct.2017.08.004.
[22] Maligno AR, Warrior NA, Long AC. Effects of interphase material properties in unidirectional fibre reinforced composites. Compos Sci Technol 2010;70:36–44. doi:10.1016/j.compscitech.2009.09.003.
[23] Wang J, Crouch SL, Mogilevskaya SG. Numerical modeling of the elastic behavior of fiber-reinforced composites with inhomogeneous interphases. Compos Sci Technol 2006;66:1–18. doi:10.1016/j.compscitech.2005.06.006.
[24] Trias D, Costa J, Mayugo JA, Hurtado JE. Random models versus periodic models for fibre reinforced composites. Comput Mater Sci 2006;Vol.38:316-324. doi.org/10.1016/j.commatsci.2006.03.005
[25] Kumar P, Chandra R, Singh SP. Effective elastic constants of fiber-reinforced polymer-matrix composites with the concept of interphase. Compos Interfaces 2010;17:15–35. doi:10.1163/092764409X12580201111502.
[26] Xu Y, Du S, Xiao J, Zhao Q. Evaluation of the effective elastic properties of long fiber reinforced composites with interphases. Comput Mater Sci 2012;61:34–41. doi:10.1016/j.commatsci.2012.03.048.
[27] Kari S, Berger H, Gabbert U, Guinovart-Diaz R, Bravo-Castillero J, Rodriguez-Ramos R. Evaluation of influence of interphase material parameters on effective material properties of three phase composites. Compos Sci Technol 2008;68:684–91. doi:10.1016/j.compscitech.2007.09.009.
[28] Wang X, Zhang J, Wang Z, Zhou S, Sun X. Effects of interphase properties in unidirectional fiber reinforced composite materials. Mater Des 2011;32:3486–92. doi:10.1016/j.matdes.2011.01.029.
[29] Liu Y, Yan Y, Yang L, She H, He M. Prediction on macroscopic elastic properties of interphase-contained long-fiber-reinforced composites and multiple nonlinear regression analysis. J Reinf Plast Compos 2012;31:1143–57. doi:10.1177/0731684412454461.
[30] Pawlik M, Dean A, Lu Y. The numerical investigation of graphene-reinforced interphase effects on the mechanical properties of carbon fibre/epoxy composites. Proc. Int. Conf. Compos. Struct. (ICCS20), 2017, p. 194–5.
[31] Johnston JP, Koo B, Subramanian N, Chattopadhyay A. Modeling the molecular structure of the carbon fiber/polymer interphase for multiscale analysis of composites. Compos Part B Eng 2017;111:27–36. doi:10.1016/j.compositesb.2016.12.008.
[32] Wacker G, Bledzki a K, Chateb A. Effect of interphase on the transverse Young's modulus of glass/epoxy composites. Compos Part A 1998;29:619–26. doi: 10.1016/S1359-835X(97)00116-4.
[33] Kundalwal SI, Ray MC. Micromechanical analysis of fuzzy fiber reinforced composites. Int J Mech Mater Des 2011;7:149–66. doi:10.1007/s10999-011-9156-4.
[34] Kulkarni M, Carnahan D, Kulkarni K, Qian D, Abot JL. Elastic response of a carbon nanotube fiber reinforced polymeric composite: A numerical and experimental study. Compos Part B Eng 2010;41:414–21. doi:10.1016/j.compositesb.2009.09.003.
[35] Chatzigeorgiou G, Seidel GD, Lagoudas DC. Effective mechanical properties of "fuzzy fiber" composites. Compos Part B Eng 2012;43:2577–93. doi:10.1016/j.compositesb.2012.03.001.
[36] Kundalwal SI, Ray MC. Effective properties of a novel continuous fuzzy-fiber reinforced composite using the method of cells and the finite element method. Eur J Mech - A/Solids 2012;36:191–203. doi:10.1016/j.euromechsol.2012.03.006.
[37] Pawlik M, Yiling Lu. Prediction of elastic constants of the fuzzy fibre reinforced polymer using computational micromechanics. IOP Conf. Ser. Mater. Sci. Eng., 2018;362(1),012006 doi.org/10.1088/1757-899x/362/1/012006
[38] Rafiee R, Ghorbanhosseini A. Stochastic multiscale modeling of randomly grown CNTs on carbon fiber. Mech Mater 2017;106:1–7. doi:10.1016/j.mechmat.2017.01.001.
[39] Rafiee R, Ghorbanhosseini A. Predicting mechanical properties of fuzzy fiber reinforced composites: radially grown carbon nanotubes on the carbon fiber. Int J Mech Mater Des 2016:1–14. doi:10.1007/s10999-016-9359-9.
[40] Hadden CM, Klimek-Mcdonald DR, Pineda EJ, King JA, Reichanadter AM, Miskioglu I, et al. Mechanical properties of graphene nanoplatelet/carbon fiber/epoxy hybrid composites: Multiscale modeling and experiments. Carbon 2015;95:100–12. doi:10.1016/j.carbon.2015.08.026.
[41] Aluko O, Gowtham S, Odegard GM. Multiscale modeling and analysis of graphene

nanoplatelet/carbon fiber/epoxy hybrid composite. Compos Part B Eng 2017;131:82–90. doi:10.1016/j.compositesb.2017.07.075.
[42] Dai G, Mishnaevsky L. Fatigue of multiscale composites with secondary nanoplatelet reinforcement: 3D computational analysis. Compos Sci Technol 2014;91:71–81. doi:10.1016/j.compscitech.2013.11.024.
[43] Mori T, Tanaka K. Average stress in matrix and average elastic energy of materials with misfitting inclusions. Acta Metall 1973;21:571–4.
[44] Ji X-Y, Cao Y-P, Feng X-Q. Micromechanics prediction of the effective elastic moduli of graphene sheet-reinforced polymer nanocomposites. Model Simul Mater Sci Eng 2010;18:045005. doi:10.1088/0965-0393/18/4/045005.
[45] Shokrieh MM, Esmkhani M, Shokrieh Z, Zhao Z. Stiffness prediction of graphene nanoplatelet/epoxy nanocomposites by a combined molecular dynamics-micromechanics method. Comput Mater Sci 2014;92:444–50. doi:10.1016/j.commatsci.2014.06.002.
[46] Shokrieh MM, Rafiee R. Stochastic multiscale modelling of CNT/polymer composites. Comput Mater Sci 2010;50:437–46. doi:10.1016/j.commatsci.2010.08.036.
[47] Giannopoulos GI, Kallivokas IG. Mechanical properties of graphene based nanocomposites incorporating a hybrid interphase. Finite Elem Anal Des 2014;90:31–40. doi:10.1016/j.finel.2014.06.008.
[48] Pontefisso A, Mishnaevsky L. Nanomorphology of graphene and CNT reinforced polymer and its effect on damage: Micromechanical numerical study. Compos Part B Eng 2016;96:338–49. doi:10.1016/j.compositesb.2016.04.006.
[49] Dai G, Mishnaevsky L. Graphene reinforced nanocomposites: 3D simulation of damage and fracture. Comput Mater Sci 2014;95:684–92. doi:10.1016/j.commatsci.2014.08.011.
[50] Cho J, Chen JY, Daniel IM. Mechanical enhancement of carbon fiber / epoxy composites by graphite nanoplatelet reinforcement Scripta Mat 2007;56:685–8. doi:10.1016/j.scriptamat.2006.12.038.
[51] Lee C, Wei X, Kysar JW, Hone J. Measurement of the elastic properties and intrinsic strength of monolayer graphene. Science 2008;321:385–8. doi:10.1126/science.1157996.
[52] Nicholl RJT, Conley HJ, Lavrik N V., Vlassiouk I, Puzyrev YS, Sreenivas VP, et al. The effect of intrinsic crumpling on the mechanics of free-standing graphene. Nat Commun 2015;6:1–7. doi:10.1038/ncomms9789.
[53] STREM Graphene Nanoplatelet https://www.strem.com/catalog/family/Graphene/ (accessed January 2, 2018).
[54] Barbero EJ. Finite Element Analysis of Composite Materials Using ANSYS. Second. CRC Press; 2014.
[55] Sun CT, Vaidya RS. Prediction of composite properties from a representative volume element. Compos Sci Technol 1996;56:171–9. doi:10.1016/0266-3538(95)00141-7.
[56] Luciano R. Variational methods for the homogenization of periodic heterogeneous media. J Mech 1998;17:599–617.
[57] Li Z, Ghosh S, Getinet N, O'Brien DJ. Micromechanical modeling and characterization of damage evolution in glass fiber epoxy matrix composites. Mech Mater 2016;99:37–52. doi:10.1016/j.mechmat.2016.05.006.
[58] ANSYS. ANSYS 2018. www.ansys.com (accessed August 10, 2018).
[59] Ding A, Li S, Wang J, Ni A, Sun L, Chang L. Prediction of Process-Induced Distortions in L-Shaped Composite Profiles Using Path-Dependent Constitutive Law. Appl Compos Mater 2016;23:1027–45. doi:10.1007/s10443-016-9501-8.
[60] BS EN ISO 14125. Fibre-reinforced plastic composites -Determination of flexural properties. vol. 1998. 1998. doi:10.1520/E0872-82R13.2.
[61] Li Z, Young RJ, Wilson NR, Kinloch IA, Valles C, Li Z. Effect of the orientation of graphene-based nanoplatelets upon the Young's modulus of nanocomposites. Compos Sci Technol 2016;123:125–33. doi:10.1016/j.compscitech.2015.12.005.
[62] Shokrieh MM, Nasir V, Karimipour H. A micromechanical study on longitudinal strength of fibrous composites exposed to acidic environment. Mater Des 2012;35:394–403. doi:10.1016/j.matdes.2011.08.044.
[63] Junhong C, Zheng B, Lu G. Vertically-Oriented Graphene: PECVD Synthesis and Applications. Springer International Publishing; 2015. doi:10.1007/978-3-319-15302-5.
[64] Madhukar MS, Drazl LT. Fiber-matrix adhesion and its effect on composite mechanical properties: I. In-plane and interlaminar shear behaviour of graphite/epoxy composites. J Compos Mater 1991;25:932-57.

List of Figures:

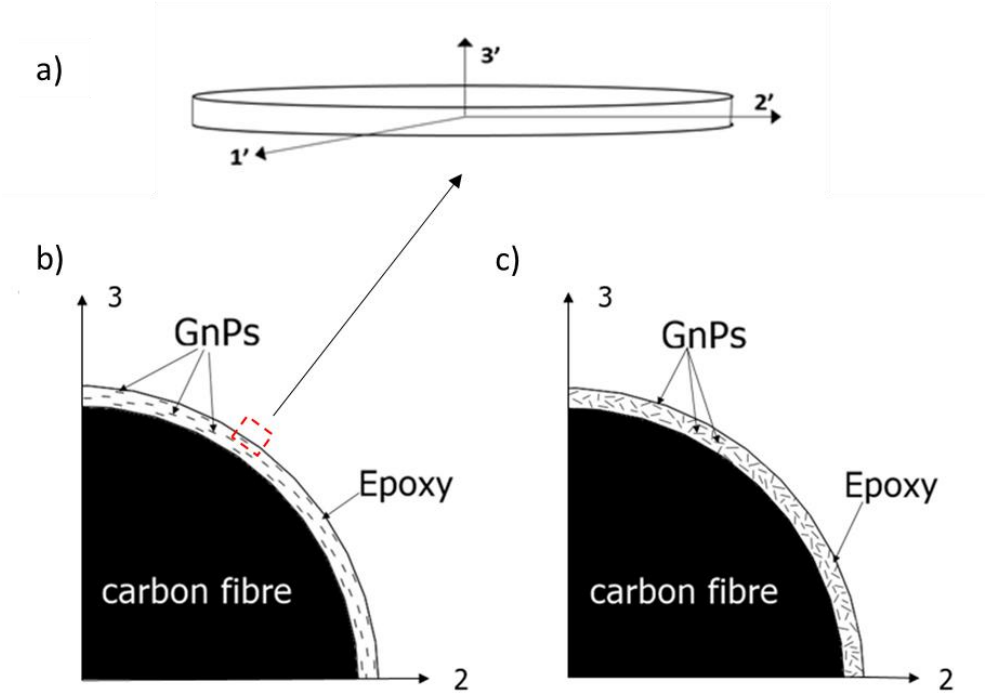

Figure 1. Schematic representations of a) single GnPs in the local coordinate system (1'-2'-3') b) a quarter of cross-section view of carbon fibre with aligned GnPs and c) a quarter of cross-section view of carbon fibre with randomly orientated GnPs within the reinforced interphase. Global coordinate system (1-2-3) is used as shown.

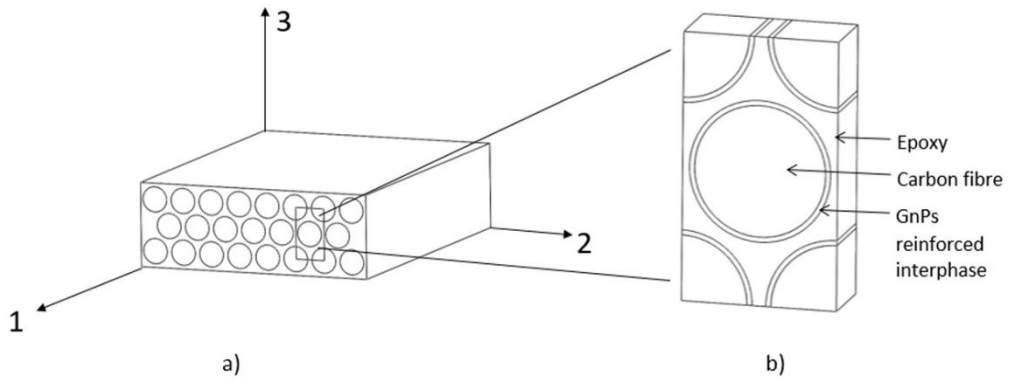

Figure 2. Schematic representations of a) unidirectional CFRP lamina b) Representative volume element model with the graphene nanoplatelets (GnPs) reinforced interphase.

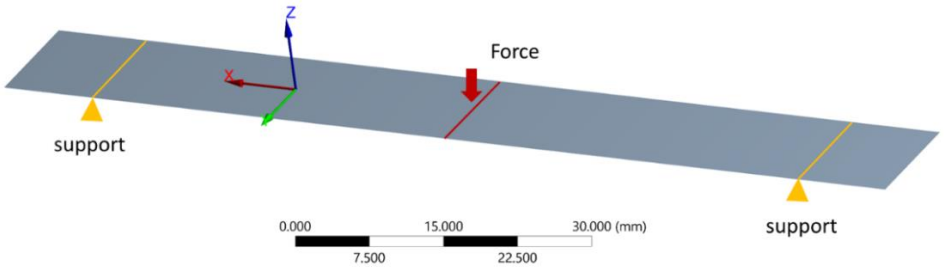

Figure 3. Boundary condition of macroscale laminate.

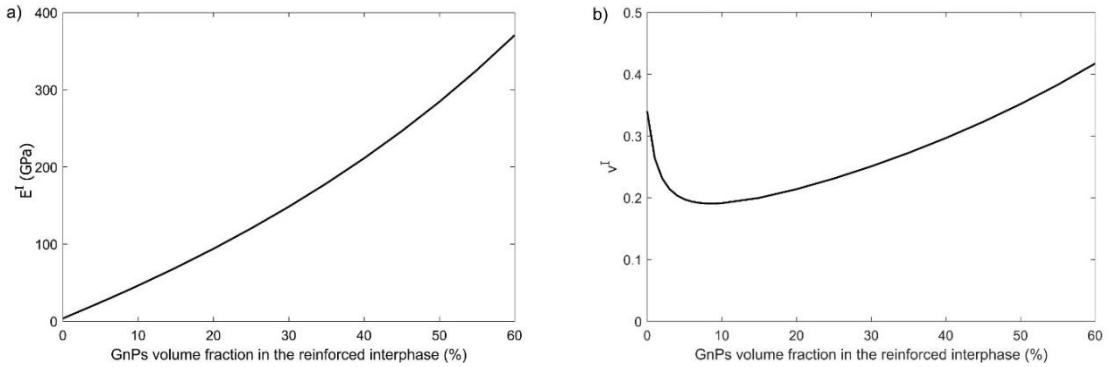

Figure 4. Mechanical properties of the reinforced interphase with randomly orientated GnPs as a function of the volume fraction of GnPs in the interphase: a) Elastic Modulus, b) Poisson's ratio.

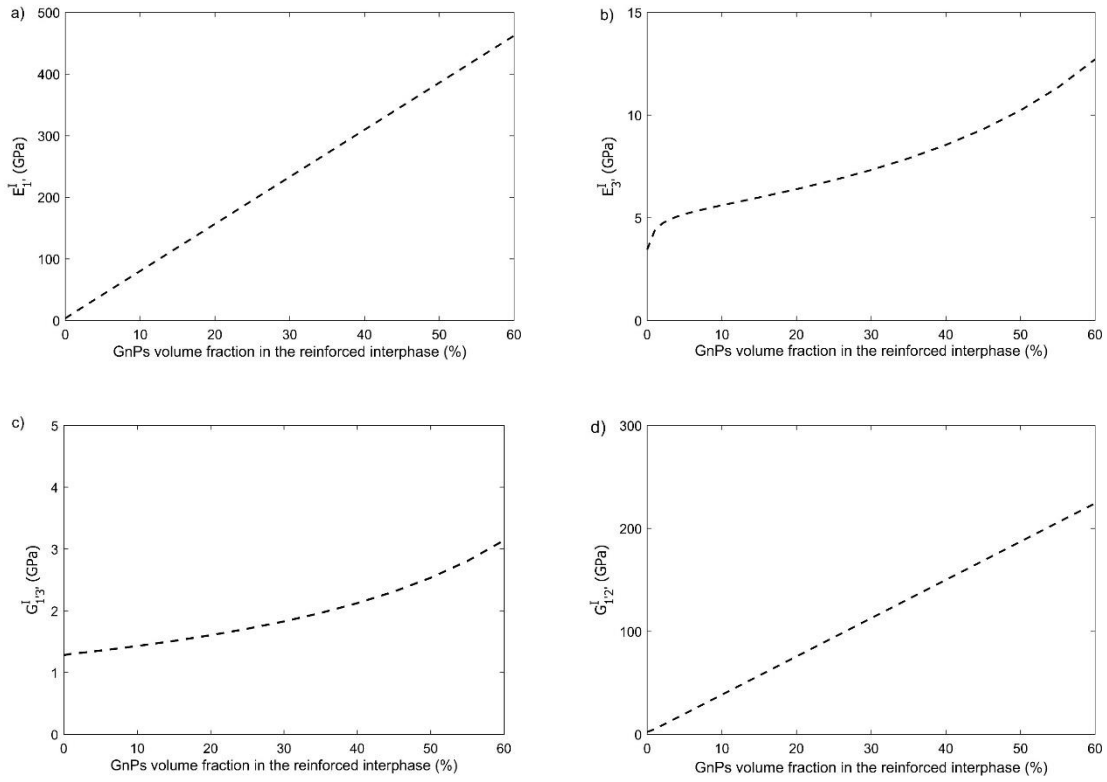

Figure 5. Mechanical properties of the reinforced interphase with aligned GnPs as a function of the volume fraction of GnPs in the interphase a) In-plane elastic modulus, b) Out-of-plane elastic modulus, and c) Out-of-plane shear modulus and d) In-plane shear modulus.

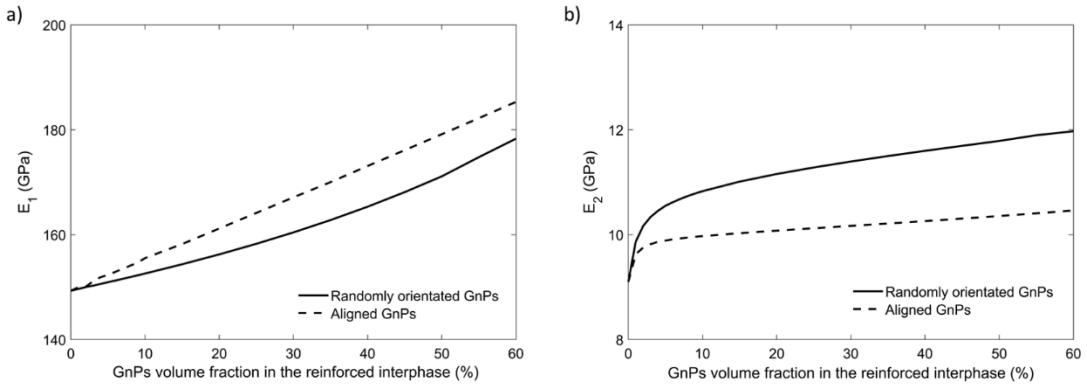

Figure 6. Effects of the volume fraction of GnPs in the reinforced interphase on elastic properties of unidirectional lamina a) longitudinal elastic modulus and b) transverse elastic modulus.

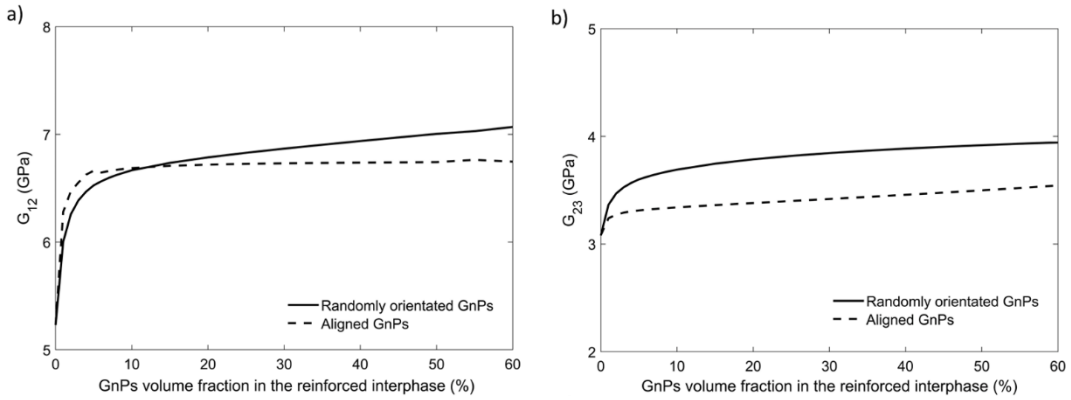

Figure 7. Effects of the volume fraction of GnPs in the reinforced interphase on shear modulus of unidirectional lamina a) longitudinal shear modulus, b) transverse shear modulus.

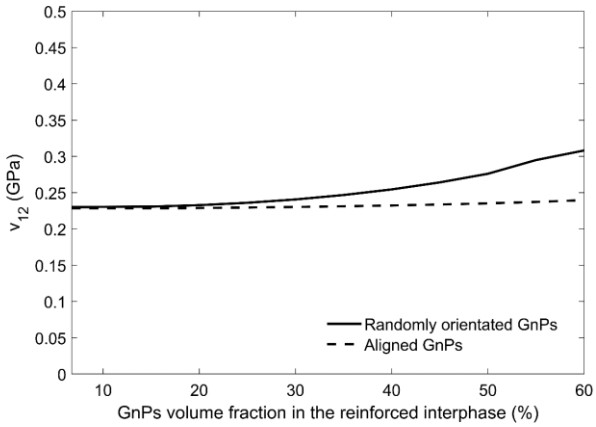

Figure 8. Effects of the volume fraction of GnPs in the reinforced interphase on longitudinal Poisson's ratio of the unidirectional lamina.

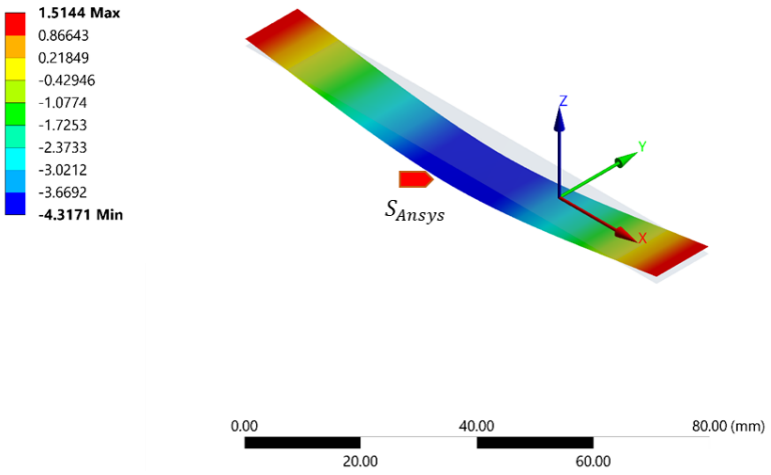

Figure 9. Example of vertical deformation contour plot in three-point bending for 0° unidirectional laminate at loading of 700 N.

List of Tables:

GnP [43]		**Carbon Fibre [59]**		**Epoxy Resin [51]**	
$E_{1'}^{r}$ (TPa)	0.77	E_1^f (GPa)	224.0	E^m (GPa)	3.45
$E_{3'}^{r}$ (TPa)	0.40	E_2^f (GPa)	17.2	v^m	0.34
$G_{1'3'}^{r}$ (GPa)	78.0	G_{12}^f (GPa)	27.6	κ^m (GPa)	3.59
$v_{1'2'}^{r}$	0.03	G_{23}^f (GPa)	5.73	μ^m (GPa)	1.28
$v_{1'3'}^{r}$	0.81	v_{12}^f	0.2		
		v_{23}^f	0.5		
		Diameter (μm)	7.1		

Table 1. Properties of GnPs, carbon fibre and matrix.

Fibre direction	**Carbon fibre AS4**	**Epoxy Resin**	**GnPs reinforced interphase**	$\boldsymbol{E_1}$ (GPa)	$\boldsymbol{E_2}$ (GPa)	$\boldsymbol{v_{12}}$	$\boldsymbol{v_{23}}$	$\boldsymbol{G_{12}}$ (GPa)
0°	65%	35%	0%	149.31	9.090	0.24	0.48	5.23
0°	66%	26.3%	7.7%	156.23	11.56	0.23	0.47	6.78

Table 2. Lamina properties predicted by RVE methods in the global coordinate system (1-2-3).

Laminate ID	**Force** $\boldsymbol{F}$ (N)	**Calculated** $\boldsymbol{E_f}$ (GPa)	**Experimental** $\boldsymbol{E_f}$ (GPa) [10]	**Percentage error** (%)
0° Control	700	143.2	139 ± 3.0	+2.92
0° GnPs	700	152.1	143 ± 9.0	+6.08
90° Control	20	8.7	8.8 ± 0.3	-0.81
90° GnPs	20	11.2	11.0 ± 0.3	+1.07

Table 3. Comparison between flexural modulus predicted by present multiscale modelling and experimental data.